Journal of Anatomy

J. Anat. (2012) **220**, pp396–404 doi: 10.1111/j.1469-7580.2011.01473.x

Morphometric analysis of intralobular, interlobular and pleural lymphatics in normal human lung

Francesca Sozio,[1,*] Antonella Rossi,[1,*] Elisabetta Weber,[1] David J. Abraham,[2] Andrew G. Nicholson,[3] Athol U. Wells,[4] Elisabetta A. Renzoni[4] and Piersante Sestini[5]

[1]*Department of Neuroscience, Molecular Medicine Section, University of Siena, Siena, Italy*
[2]*Centre for Rheumatology and Connective Tissue Diseases, UCL Medical School, London, UK*
[3]*Department of Histopathology, Royal Brompton Hospital, London, UK*
[4]*Interstitial Lung Disease Unit, Royal Brompton Hospital, London, UK*
[5]*Department of Clinical Medicine and Immunological Sciences, Section of Respiratory Diseases, University of Siena, Siena, Italy*

Abstract

In spite of their presumed relevance in maintaining interalveolar septal fluid homeostasis, the knowledge of the anatomy of human lung lymphatics is still incomplete. The recent discovery of reliable markers specific for lymphatic endothelium has led to the observation that, contrary to previous assumptions, human lymphatic vessels extend deep inside the pulmonary lobule in association with bronchioles, intralobular arterioles or small pulmonary veins. The aim of this study was to provide a morphometric characterization of lymphatic vessels in the periphery of the human lung. Human lung sections were immunolabelled with the lymphatic marker D2-40, followed by blood vessel staining with von Willebrand Factor. Lymphatic vessels were classified into: intralobular (including those associated with bronchovascular bundles, perivascular, peribronchiolar and interalveolar), pleural (in the connective tissue of the visceral pleura), and interlobular (in interlobular septa). The percentage area occupied by the lymphatic lumen was much greater in the interlobular septa and in the subpleural space than in the lobule. Most of the intralobular lymphatic vessels were in close contact with a blood vessel, either alone or within a bronchovascular bundle, whereas 7% were associated with a bronchiole and < 1% were not connected to blood vessels or bronchioles (interalveolar). Intralobular lymphatic size progressively decreased from bronchovascular through to peribronchiolar, perivascular and interalveolar lymphatics. Lymphatics associated with bronchovascular bundles had similar morphometric characteristics to pleural and interlobular lymphatics. Shape factors were similar across lymphatic populations, except that peribronchiolar lymphatics had a marginally increased roundness and circularity, suggesting a more regular shape due to increased filling, and interlobular lymphatics had greater elongation, due to a greater proportion of conducting lymphatics cut longitudinally. Unsupervised cluster analysis confirmed a marked heterogeneity of lymphatic vessels both within and between groups, with a cluster of smaller vessels specifically represented in perivascular and interalveolar lymphatics within the alveolar interstitium. Our data indicate that intralobular lymphatics are a heterogeneous population, including vessels surrounding the bronchovascular bundle analogous to the conducting vessels present in the pleural and interlobular septa, many small perivascular lymphatics responsible for maintaining fluid balance in the alveolar interstitium, and a minority of intermediate lymphatics draining the peripheral airways. These lymphatic populations could be differentially involved in the pathogenesis of diseases preferentially involving distinct lung compartments.

Key words: D2-40; immunohistochemistry; lung; lymphatic vessels; morphometric analysis.

Introduction

Lymphatic vessels of the lung participate in essential functions such as adaptation to air breathing at birth (Kulkarni et al. 2011), control of interstitial fluid, inflammatory and immune responses (Schraufnagel, 2010), and possibly tissue repair and fibrosis (El-Chemaly et al. 2009). Due to their thin wall structure, lack of reliable morphological markers and complex interconnections, the study of their anatomy has been limited for many years to methods based on experimental filling, such as India ink or fluorescent dyes or, more recently, scanning electron microscopy inspection of casts (Ohtani & Ohtani, 2008; Schraufnagel, 2010). It has long been assumed that most lung lymphatic vessels extend within the connective tissue sheets surrounding airways and blood vessels (Lauweryns & Baert, 1977; Marchetti et al.

Correspondence
Elisabetta Renzoni, Interstitial Lung Disease Unit, Emmanuel Kaye Building, 1B Manresa Rd, London SW3 6LR, UK.
E: e.renzoni@imperial.ac.uk
*These authors contributed equally to this work.

Accepted for publication *28 December 2011*
Article published online *30 January 2012*

1994). In line with recent findings on their ontogeny, it has been shown in the rat that lymphatic endothelial cells cluster first in the primary region and then along secondary broncho-arterial regions and veins (Kulkarni et al. 2011). However, most observations on this subject are in animals and the knowledge of the anatomy of lung lymphatics in humans is still incomplete.

The recent identification of relatively specific lymphatic molecular markers, coupled with the availability of immunochemical reagents for their visualization, has allowed a greater understanding of the lymphatic system (Kahn & Marks, 2002; Scavelli et al. 2004; Kato et al. 2006). Using anti-podoplanin antibodies, Kambouchner & Bernaudin (2009) have demonstrated that, contrary to what was generally assumed, human lymphatic vessels extend beyond the respiratory bronchioles, accompanying intralobular arteries deep inside the lobule (secondary lobule, Hansell et al. 2008), and that some are present even independently of blood vessels, in the inter-alveolar septa. This finding extends the possible role of lymphatics in this delicate district of the lung, particularly in response to increased interstitial fluid, inhaled pollutants and in the context of interstitial lung diseases (Schraufnagel, 2010).

The lobule, defined as the smallest unit of lung structure marginated by connective tissue septa (interlobular septa), is supplied by a centrally located bronchiole and pulmonary artery branch. The two form a bronchovascular bundle, which is surrounded by a small amount of supporting connective tissue. The pulmonary artery branch gives rise to arterioles, which in turn feed the rich capillary network in the interalveolar septa. Small venules carry the oxygenated blood towards the periphery of the lobule, merging into the pulmonary vein branches that run in the interlobular septa, together with lymphatics. The lobule also contains terminal (with a continuous wall) and respiratory bronchioles (with the wall interrupted by alveoli), accompanied by small bronchial arteries, derived from the thoracic aorta, which supply the bronchiole wall with oxygen and nutrients, and small bronchial veins which will ultimately drain mainly into the pulmonary veins. Whereas lung blood vessels associated with intralobular lymphatics have been characterized according to their diameter (Kambouchner & Bernaudin, 2009), the morphological characteristics and the distribution of the lymphatics associated with the lobule have not yet been fully described and compared with lung lymphatics of other districts.

In this study, we provide a morphometric characterization of the lymphatic vessels of human lung tissue, analysing the lymphatics present at different levels within the lobule and comparing them with the lymphatic vessels of other lung compartments, such as the interlobular septa and the pleural connective tissue. The aim of the study is to provide a quantitative assessment of their distribution as a rational basis for their presumed relevance in maintaining the pulmonary interstitial spaces free of excess fluid.

Patients, materials and methods

Patients

Normal lung at the periphery of resected cancer was obtained from five patients undergoing lung cancer resection surgery at the Royal Brompton Hospital, London, following informed consent and ethical approval. Mean age was 63 years (range 35–80 years). None of the patients suffered from heart failure or hypoalbuminaemia. Resected cancers included two squamous carcinomas, two adenocarcinoma, and one metastatic leiomyosarcoma. Two of the samples were derived from the left lower lobe, and one each from the right lower lobe, the left upper lobe, and the right middle lobe. All sections of normal lung were taken in areas remote from the cancer, so that there was no cancer tissue or surrounding stromal tissue in any of the investigated sections. The diaphragmatic pleura was avoided. All sections of normal lung were identified by an experienced lung pathologist (A.G.N.).

Immunostaining

Biopsies were fixed in 10% formalin and embedded in paraffin. After rehydration in graded alcohol series, sections were placed for 10 min in boiling Antigen Unmasking Solution (Vector Laboratories, Burlingame, CA, USA) for antigen retrieval. Endogenous peroxidase activity was quenched with 3% H_2O_2 for 15 min in the dark and unspecific binding sites were blocked for 30 min with phosphate-buffered saline (PBS) containing 3% bovine serum albumin (BSA). Double labelling was performed by the sequential use of the monoclonal antibody D2-40 (Signet) that specifically stains lymphatic vessels (Kahn & Marks, 2002) and a polyclonal antibody to von Willebrand Factor (vWF; Dako), expressed by blood endothelium and, to a lesser extent, by lymphatic endothelium. Lymphatic vessels were stained by incubating sections for 2 h at room temperature with D2-40 diluted 1 : 40 in PBS containing 0.5% BSA (hereafter referred to as buffer), followed by 30 min incubation with anti-mouse IgG (DakoCytomation, Glostrup, Denmark) diluted 1 : 25 in buffer, and eventually 30 min with peroxidase-antiperoxidase (PAP-mouse, Dako) diluted 1 : 100 at room temperature. The reaction was revealed with the 3,3′-diaminobenzidine Substrate Kit for Peroxidase (Vector), which contains a nickel solution that converts the brown colour characteristic of 3,3′-diaminobenzidine to black. Blood vessels were then stained by overnight incubation at 4 °C with the polyclonal antibody to vWF (1 : 50), followed by a 45-min incubation at room temperature with anti-rabbit/alkaline phosphatase (AP, Dako) (1 : 50). The reaction was visualized with Fuchsin Substrate-Chromogen System (Dako). Sections were counterstained with toluidine blue. Double labelling allowed distinction of lymphatic vessels, stained in black by DAB and nickel, from blood vessels, stained in red by fuchsine.

Morphometric analysis

Samples were viewed under a Nikon Eclipse E600 light microscope equipped with a digital camera and morphometric analysis was performed using the morphometric software NIS ELEMENTS by Nikon.

Using a × 10 objective lens, the entire pleura, the entire area occupied by interlobular septa, five fields of tissue containing bronchovascular bundles, and 50 random fields of peripheral lung tissue excluding areas containing pleura, interlobular septa or bronchovascular bundles were photographed for each biopsy. Bronchovascular bundles were composed of a bronchiole with a diameter > 200 μm (range 220–800 μm, mean 473 μm), accompanied by a pulmonary artery branch with a diameter > 150 μm (range 160–800 μm, mean 322 μm). Bundles are found at the centre of lobular and acinar structures. As they were relatively scanty in the biopsies, we decided to measure them in specifically focused fields. The number of five fields was chosen as the maximum number of fields obtainable in all the sections. The total area occupied by lung parenchyma was automatically calculated by the software by selecting the thresholds of all the colours present in each photographic field. Spaces containing air were thus excluded. The areas occupied by pleural tissue and by interlobular septa were measured with the help of a graphic tablet. The mean area examined for each of these compartment was 3.9 ± 0.5 mm^2 (M ± SE) in the random fields, 2.4 ± 1.6 mm^2 in intralobular septa, and 2.2 ± 0.8 mm^2 in pleural tissue. Due to their relatively large size, the area of bronchovascular bundles was not measured, as it was impossible to delimit it entirely in most of the photographic fields examined.

The luminal area of lymphatic vessels was automatically calculated by the software by manually tracing their inner perimeter with a graphic tablet (Rossi et al. 2010). The following shape form factors were calculated: roundness (Cox, 1927), defined as the square of the ratio of the radius of a circle having the same perimeter as the vessel over the radius of a circle having the same area, computed as $4\pi a/p2$ (where a and p are the area and the perimeter, respectively); ellipse axis ratio, defined as the ratio between the major and minor axis of an ellipse having the same area and perimeter as the vessel. Both parameters are 1 in the case of a perfect circle and decrease departing from circularity; elongation, which is computed as max feret per min feret (the maximum and minimum length, respectively, for all orientations), is 1 for a regular shape and increases as the shape increases along one dimension. Vessel density was expressed as the total number of vessels identified in each field, divided by the tissue area in mm^2, and vessel area as the percentage of the sum of the areas of all vessels over tissue area.

Lymphatic vessels were classified into pleural (in the connective tissue of visceral pleura), interlobular (in the interlobular septa), and intralobular. These were further subdivided into bronchovascular (associated with a bronchiolo-arterial bundle), perivascular (at < 100 μm from a blood vessel with at least 15 μm diameter, but at more than 100 μm from a bronchiole), peribronchiolar (at < 100 μm from a bronchiole, and, at times, also at < 100 μm from a small blood vessel, but with the bronchiole and the vessel not forming part of an identifiable bronchovascular bundle), and interalveolar (within the alveolar walls, at a distance > 100 μm from the closest bronchiole or blood vessel). Peribronchiolar, perivascular and interalveolar lymphatics were identified and measured in the random fields, whereas the bronchovascular lymphatics were measured in the microscopic fields specifically aimed at the bronchovascular bundles. Interlobular septa were missing in two specimens.

We measured the smaller diameter of blood vessels (from the external elastic lamina of one side to the external elastic lamina of the other, as reported by Schermuly et al. 2005), to avoid artefacts due to the possible obliquity of the section plane with respect to the vessel. Only blood vessels with a luminal diameter > 15 μm were evaluated, regardless of the intensity of the vWF staining. We chose this parameter to be sure to positively exclude blood capillaries, which usually have a much smaller diameter (< 10 μm).

Statistical analysis

Means and robust standard errors were computed using generalized linear models, using Gaussian family and identity link and including the subject as a random effect variable. Logarithmic transformation was applied when needed, to improve normality of the data distribution and the homoscedasticity of variances. For statistical comparisons, the relevant factors were added to the model as fixed effect variables. Simulation experiments indicated that with a sample size of 30 lymphatics of a given type for each of five patients, the analysis had a power of 80% of detecting a difference of 15% between two means with an α of 0.05 (Feiveson, 2002). Lymphatic density and percentage of tissue area occupied by lymphatic lumens in each subject were analysed by one-way analysis of variance, followed by Scheffé test for multiple comparisons. A P value ≤ 0.05 according to a two-tail distribution was considered statistically significant (STATA statistical software: Release 9. StataCorp LP, College Station, TX, USA).

To validate our classification based on the proximity to different anatomical structures, we compared it with an alternative classification identified by unsupervised cluster analysis of the morphometric data (Sokal, 1974). We first performed a dimensionality reduction through principal component analysis using the following list of parameters: perimeter, area, max feret, min feret (all log-transformed), ellipse axis ratio, roundness and elongation. The first relevant components were retained based on inspection of the scree plot (Supporting Information Fig. S3) and were subjected to a non-hierarchical k-medians cluster analysis, yielding a classification of individual vessels over five mutually exclusive clusters. This method generates clusters in a top-down manner for a given number of clusters. The positions of the cluster centroids are at first randomly generated and then iteratively optimized until they converge to a stable position. The classification thus obtained was compared with our original classification by computing the percentage of lymphatics belonging to each cluster among the different populations of intralobular, pleural and interlobular lymphatics.

Results

Immunohistochemistry

The endothelium of lymphatic vessels showed intense immunostaining for D2-40. Type 2 pneumocytes were stained by D2-40 to a much lesser extent. The great majority of lymphatic vessels, whether associated with bronchovascular bundles or not, were present in the interstitium encircling arteries or arterioles (Fig. 1A–C). Arteries present in the section (with a diameter between the external elastic lamina of both sides > 100 μm) were almost always accompanied by a conductive airway (usually a bronchiole in the biopsies, which were all peripheral) in a bronchovascular bundle. The lymphatics

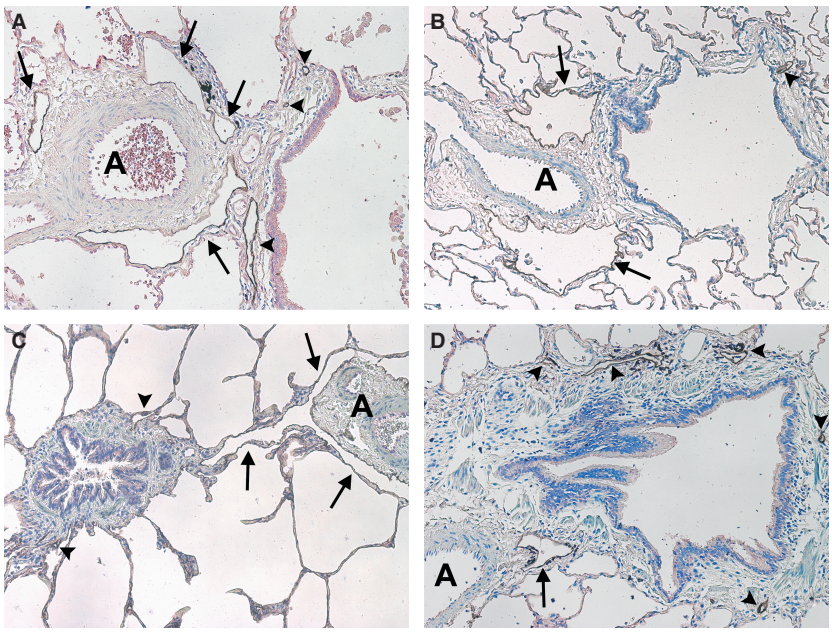

Fig. 1 Intralobular lymphatic vessels associated with bronchovascular bundles. Large lymphatic vessels (arrows) around the arteries (A–C), also occupying the space between the artery and the bronchus or bronchiole (A, C and D). The lymphatic vessels specifically associated with conductive airways (arrowheads) are much smaller. Original magnification × 10.

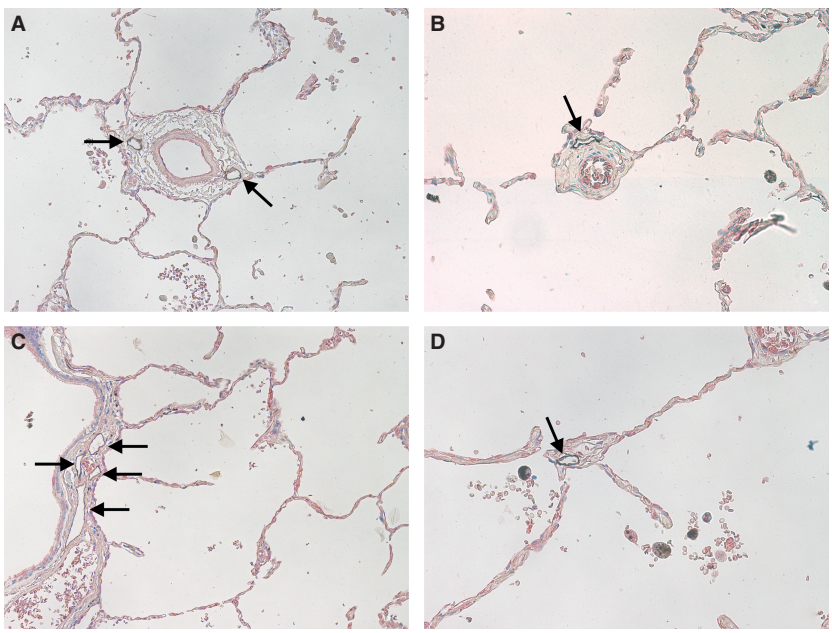

Fig. 2 Intralobular lymphatics in random fields. Most of intralobular lymphatic vessels were associated with small arteries (A) or arterioles (B). Some were associated with bronchioles (C); the small vessel at the bottom left of the field is a venule. True interalveolar lymphatics (D), not associated with a blood microvessels or a bronchiole, were extremely small and rare. Original magnification × 10.

located in the connective space between the artery and the bronchus were usually larger than those located on the bronchial side opposite to the artery (Fig. 1A–D).

The photographic fields randomly selected from the peripheral lung contained small blood vessels, mainly arterioles with a diameter of < 100 μm, and a few bronchioles (terminal or respiratory), generally of much larger dimensions (250–500 μm). Lymphatic vessels associated with parenchymal arteries (Fig. 2A) and arterioles (Fig. 2B) were smaller than those associated with bronchioles (Fig. 2C). Only a few tiny lymphatic vessels were not associated with blood vessels and were classified as true interalveolar (Fig. 2D).

Long lymphatic vessels (Fig. 3A), often provided with valves, were seen in the interlobular septa together with pulmonary veins (Fig. 3B). The lymphatics of interlobular septa were connected with pleural lymphatics (Fig. 3C). Pleural lymphatics (Fig. 3d) were numerous and large. They were located in the connective tissue of the visceral pleura, adjacent to the lung parenchyma.

Morphometric analysis

Lymphatics were identified in 195/233 random fields (84%), with a density of 26 ± 4 vessels per mm^2 and occupying 0.9 ± 0.2% of the tissue surface with their lumen. By

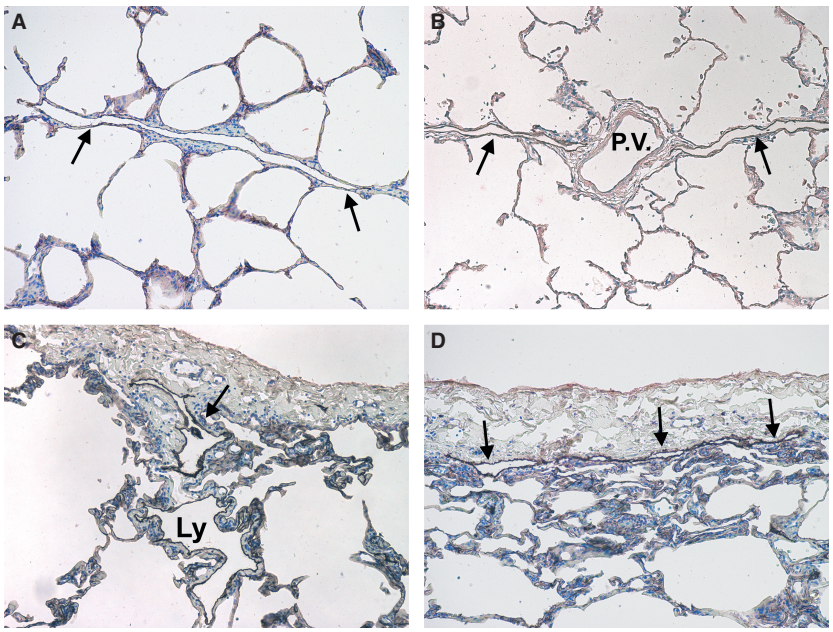

Fig. 3 Lymphatics of the interlobular septa and the visceral pleura. (A) A long lymphatic vessel in an interlobular septum; (B) two lymphatic vessels (arrows) and a pulmonary vein branch (P.V.) in an interlobular septum; (C) an interlobular lymphatic (Ly) connecting with a pleural one (arrow); (D) long pleural lymphatics in the deepest part of visceral pleura along pulmonary parenchyma. Original magnification × 10.

comparison, blood vessel density was 71 ± 4 vessels per mm^2. Most of the lymphatic vessels (93%) were in close contact with a small blood vessel (in 98% of cases, the diameter was < 50 μm), 7% were close to a bronchiole (Fig. 2C) (with or without an identifiable accompanying blood vessel). The mean dimensions of perivascular lymphatics in each patient are reported in Table S1 of the Supporting Information.

The distribution of the area and the perimeter of the four types of lymphatic vessels was markedly skewed, as shown in Fig. 4. A logarithmic transformation resulted in a reasonably normal distribution (Supporting Information Fig. S1), and statistical analysis was therefore performed on log-transformed data. The mean area and perimeter of the three interalveolar lymphatics was 53 (95% CI 41–68) μm^2, and 40 μm (35–46), respectively. Due to their small number, they were omitted from statistical analysis. Geometric means of the other groups are reported in Table 1. No differences were observed in mean area or perimeter between bronchovascular pleural and interlobular lymphatics. Peribronchiolar lymphatics were found to be significantly smaller than the bronchovascular ones, (perimeter, $P \sim 0.05$, area: $P = 0.045$, min feret $P = 0.036$) and to have greater ellipse axis ratio ($P = 0.018$) and roundness ($P = 0.021$). In turn, all dimensional parameters, including area, perimeter, min feret and max feret of perivascular intralobular lymphatics were much smaller than bronchovascular and peribronchiolar lymphatics ($P < 0.00001$ for both comparisons). Shape factors were similar to bronchovascular lymphatics, whereas peribronchiolar lymphatics tended to be rounder. All the morphometric parameters of pleural and interlobular lymphatics were similar to those of lymphatics associated with bronchovascular bundles, except for a greater elongation in pleural vessels, reflecting an increased percentage of vessels with a high elongation value, > 6 (21 vs. 6–11% in the other groups, $P = 0.033$; Supporting Information Fig. S2).

Adjusting for multiple comparisons, no significant differences were observed in the density of lymphatic vessels between the intralobular tissue, the interlobular septa and the subpleural spaces, although a trend toward a lower density was observed in pleural lymphatics. However, the percentage of the area occupied by lymphatics was significantly different in the three compartments, being greater in the septa than in subpleural spaces ($P = 0.011$) and in these with respect to intralobular tissue ($P = 0.034$).

Cluster analysis

The principal component analysis yielded seven components, four of which were retained based on inspection of the scree plot. The principal-component loading matrix and the scree plot of eigenvalues are presented in Table S2 of the Supporting Information. The mean values of the full list of morphometric parameters in the five cluster types identified by cluster analysis are reported in Table 2.

It is apparent that Cluster 5 recognizes small lymphatics, Cluster 4 large lymphatics, Cluster 3 lymphatics with a relatively regular shape, Cluster 2 more elongated lymphatics, and Cluster 1 medium-sized lymphatics. The correspondence between the computer-generated classification and our original classification is shown in Table 3.

Perivascular lymphatics are characterized by the presence of a greater proportion of Cluster 5 (small) lymphatics and very few Cluster 4 (large) vessels, bronchovascular and pleural lymphatics have a very similar composition, peribronchiolar lymphatics have a somewhat intermediate

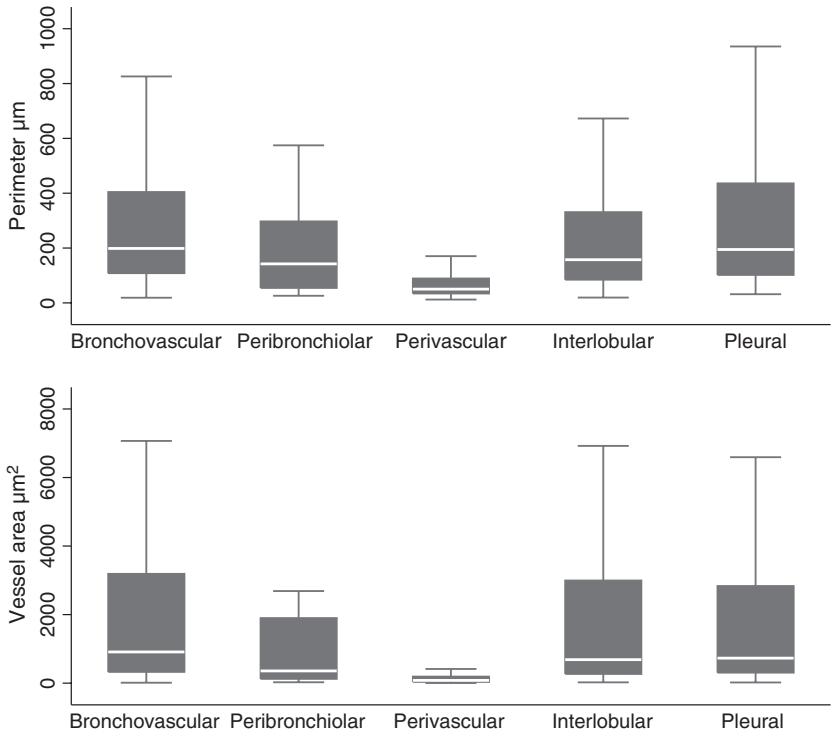

Fig. 4 Box and whisker plots of the untransformed perimeter (upper panel) and area (lower panel) of different populations of lymphatic vessels. The central bar represents the median, the box the lower and upper quartiles, and the whiskers the more extreme data within 1.5 interquartile ranges of the upper and of the lower quartiles. Note the smaller dimensions of perivascular intralobular lymphatics and the skewed distribution in all the groups.

Table 1 Mean values of the morphometric parameters of different groups of lymphatic vessels.

	Bronchovascular bundles	Peribronchiolar	Perivascular	Pleural	Interlobular
N	122	30	463	181	146
Area μm^2	1024 (574–1826)	522 (435–626)*	88 (60–129)*	864 (597–1249)	841 (797–888)
Perimeter μm	200 (157–256)	139 (114–169)*	58 (47–73)*	209 (151–289)	175 (148–207)
Roundness	0.39 ± 0.04	0.44 ± 0.04*	0.38 ± 0.02	0.37 ± 0.06	0.41 ± 0.04
Ellipse axis ratio	0.21 ± 0.02	0.25 ± 0.03*	0.21 ± 0.02	0.21 ± 0.04	0.22 ± 0.03
Elongation	3.2 ± 0.2	3.6 ± 0.2	3.4 ± 0.1	4.5 ± 0.7*	3.4 ± 0.4
Max Feret μm	79 (61–102)	55 (48–64)*	24 (19–29)*	86 (61–121)	71 (59–84)
Min Feret μm	28 (21–36)	20 (16–24)	8 (7–10)*	25 (21–29)	24 (23–25)
Density (mm^{-2})	ND	25 ± 4		14 ± 2	27 ± 6
% area	ND	1.2 ± 0.3*		4.2 ± 0.7*	8.6 ± 1.4*

ND, not determined.
*Statistically significant (see text).
Data presented either as M ± SE or as geometric mean (GM) with 95% CI in parenthesis, as appropriate.

composition, and pleural lymphatics have the greater percentage of elongated Cluster 2 vessels. The three interalveolar lymphatics were all classified as cluster 5 (not shown).

Discussion

Lymphatic vessels in the human lung have only recently been shown to extend within the lobule beyond respiratory bronchioles or their satellite arteries (Kambouchner & Bernaudin, 2009). Our data confirm these findings and further provide evidence for heterogeneity of lymphatic vessels within the lobule, in comparison with lymphatics from other lung districts, which is likely to reflect functional differences.

We found that the size of lymphatic vessels, like that of bronchial structures and blood vessels, decreases moving to the periphery of lung parenchyma. At all levels, however, most of the lung lymphatics surround the arteries (Kambouchner & Bernaudin, 2009), either associated with conductive airways to form bronchovascular bundles or not. This is probably due to the fact that the arterial wall (both endothelial and smooth muscle cells) expresses the main lymphangiogenic factor, vascular endothelial growth factor C (VEGF-C; Partanen et al. 2000), which would promote

Table 2 Mean values of morphometric parameters of different groups of lymphatic vessels identified by cluster analysis.

	Cluster 1	Cluster 2	Cluster 3	Cluster 4	Cluster 5
N	200	145	197	152	251
Area μm^2	649 (586–720)*	373 (314–443)	106 (93–121)	6252 (5418–7214)	40 (36–45)
Perimeter μm	139 (132–146)	207 (187–228)	44 (42–47)	581 (536–630)	42 (40–44)
Roundness	0.45 ± 0.01	0.13 ± 0.01	0.69 ± 0.01	0.28 ± 0.01	0.32 ± 0.01
Ellipse axis ratio	0.24 ± 0.0	0.07 ± 0.01	0.41 ± 0.01	0.14 ± 0.01	0.16 ± 0.01
Elongation	2.6 ± 0.1	7.3 ± 0.3	1.9 ± 0.4	3.5 ± 0.1	3.7 ± 0.1
Max Feret μm	55 (52–58)	92 (83–102)	17 (16–18)	223 (206–242)	17 (16–18)
Min Feret μm	22 (21–23)	14 (13–16)	9 (8–10)	71 (65–77)	5 (4–6)

*GM (95% CI).

Table 3 Distribution of lymphatic vessels belonging to different morphometric clusters among different groups of lung lymphatics.

	Cluster 1 (%)	Cluster 2 (%)	Cluster 3 (%)	Cluster 4 (%)	Cluster 5 (%)
Bronchovascular bundles	34	14	12	33	7
Peribronchiolar	23	20	27	27	3
Perivascular	12	12	26	3	47
Interlobular	35	14	18	28	5
Pleural	24	25	16	26	8

lymphatic vessel formation during development (Jurisic & Detmar, 2009). In an elegant *in vitro* experiment, Kriehuber et al. (2001) have shown that lymphatic and blood endothelial cells seeded in matrigel form independent capillary tubes that wind around each other, suggesting that this peculiar arrangement may be due to VEGF-C production by blood endothelial cells. Gene array studies have indeed identified VEGF-C gene expression in cultured blood endothelial cells (Hirakawa et al. 2003). The preferential arrangement of lung lymphatics around pulmonary artery branches is similar to what has been reported in other anatomic districts, including the liver (Comparini, 1969), pancreas (O'Morchoe, 1997) and kidney (Bonsib, 2006; Lee et al. 2011). As the lymphatic system lacks a propulsive force comparable to the heart pump in the blood circulation, arterial pulsation, together with respiratory and cardiac movements, may be relevant in promoting lymph progression in the lung.

The reasons for the larger size of the relatively few lymphatics observed in proximity of the bronchiolar walls compared to the perivascular lymphatics may be twofold. On the one hand, it may reflect a greater availability of lymphangiogenic factors, as the airway epithelium is, at least in the mouse, an additional source of VEGF-C (Baluk et al. 2005), which could explain the observation of lymphatics not invariably associated with blood vessels. On the other, it may simply be a consequence of peribronchiolar lymphatics being more proximal than those only in contact with blood vessels, representing branches intermediate between those reabsorbing fluid from the alveolar interstitium and the larger conducting vessels of the bronchovascular bundle. The small increase in roundness and ellipse axis ratio of these vessels supports the hypothesis that they might be more filled, possibly collecting fluid from the more numerous small lymphatic vessels downstream in the lobular interstitial spaces and/or from the airways.

Very few lymphatics are found in the interalveolar septa. Most are strictly associated with small blood vessels with a diameter > 15 μm. Interalveolar lymphatics, due to their small size and number, probably do not play a significant role in the interstitial drainage of the lung under normal conditions. It is worth considering that pulmonary interstitial fluid is very scant under normal conditions: several physiologic mechanisms including the so-called tissue safety factor (a low tissue compliance mainly due to hyaluronan and proteoglycans) and low microvessel permeability, maintain the pulmonary interstitium dehydrated at subatmospheric pressure, preventing pulmonary oedema, which would engulf the alveolo-capillary barrier and hamper gas diffusion (Miserocchi et al. 2001; Negrini & Passi, 2007). Interalveolar lymphatics may become functionally more relevant in chronic inflammation, when they may be the source of newly formed lymphatics (El-Chemaly et al. 2009; Yamashita et al. 2009).

The proportion of area occupied by lymphatics was greatest in the interlobular septa, followed by the subpleural space, both significantly greater than the area occupied by lymphatic vessels in the intralobular tissue.

The long lymphatics, with the appearance of conducting vessels running within interlobular septa (Fig. 3A), together with pulmonary vein branches, are connected with pleural lymphatics, located in the connective tissue of the visceral pleura adjacent to lung parenchyma. Overall, we found no differences in the morphometric characteristics between bronchovascular, pleural and interlobular lymphatics, except that the pleural lymphatics were more frequently cut longitudinally, possibly as a result of the linear course of the pleura where they are contained. Pleural lymphatics resemble conducting rather than absorbing structures, in line with the present general belief that they only play a minor role in the absorption of pleural fluid (Zocchi, 2002; Lai Fook, 2004).

Our classification was consistent with the results of an unsupervised cluster analysis based on morphometric data. Principal component analysis and cluster analysis have the potential of detecting differences or correlations in the data which may escape the human observer, and have been proven to be valuable classification tools in a variety of fields (Sokal, 1974), including morphometric studies (Karagiannis et al. 2009). Unsupervised clustering algorithms take simultaneously into account the numerous features determined for each vessel, allowing a polythetic classification scheme (that is, with elements of each class having many, but not all, properties in common). The concordance between our monothetic classification based on the proximity to different anatomical structures and the polythetic classification based on a variety of morphometric data, supports the notion of lymphatic heterogeneity within the lobule. We cannot exclude, however, that additional measurements or markers (Wick et al. 2008) could further improve the classification of lung lymphatics. Nevertheless, this analysis shows that not only are there differences in morphometric characteristics between lymphatics of distinct lung compartments, but also suggests a certain degree of heterogeneity of lymphatic vessels within each of the different compartments. Thus, even if perivascular lymphatic vessels were found to be markedly smaller than the other groups, only about 50% of them belong to the cluster specific for small vessels. On the other hand, very few of these small lymphatics are found outside this compartment, suggesting a specific functional role of these vessels in the fluid balance control of the alveolar interstitium.

Lymphatic measurements could have been affected by a number of factors, including the apical/basal location, mechanical ventilation pressures during surgery, or sample processing including differing degrees of compression/collapse. The number of samples was too small to adjust for lobe of provenance. All samples were well removed from the cancer tissue, resections were performed using standardized ventilation procedures, and samples underwent standard inflation/fixation procedures (Corrin et al. 2011) which would be expected to provide uniform expansion of the parenchyma. Nevertheless, if present, misclassification would be expected to reduce, rather than increase, the significance of any observed difference (Mote & Anderson, 1965).

This study provides a morphometric characterization of lymphatics in the lung periphery. Within the intralobular lymphatics recently described in normal human lung by Kambouchner & Bernaudin (2009), we identified three different populations of lymphatic vessels, defined by their vicinity to other tissue structures and characterized by different morphometric parameters. Lymphatics associated with the bronchovascular bundle have similar characteristics to the conducting lymphatics of the subpleural space and interlobular septa, while perivascular lymphatics are smaller structures, located more peripherally along the lobule, and constitute the great majority of the lymphatic vessels in the lung. Peribronchiolar lymphatics have intermediate characteristics between these two populations, and might represent connecting structures between the two. Due to their small number, we weren't able to establish whether interalveolar lymphatics are a fourth population with distinct morphometric characteristics from the perivascular lymphatics. The role of lymphatic vessels and lymphangiogenesis in the pathogenesis of different lung diseases has recently attracted growing interest (El Chemaly et al. 2008), with several diseases analysed in relation to different lymphatic compartments, as categorized above: peribronchial lymphatics in mouse models of asthma and mycoplasma infection (Aurora et al. 2005; Ebina, 2008), small peripheral lymphatics in diffuse alveolar damage (Mandal et al. 2008, Yamashita et al. 2009) and in sarcoidosis (Kambouchner et al. 2011), lymphatics of the interlobular septa in idiopathic pulmonary fibrosis (Ebina et al. 2010). Thus, we propose that the classification of lung lymphatics resulting from our morphometric analysis could be useful in the investigation of the role of lymphatic vessels in the normal lung, as well as in disease.

Acknowledgements

This work was supported by the University of Siena (Progetto di Ateneo per la Ricerca) and by MIUR Project No. 2008W7XP29.

Author contribution

Francesca Sozio and Antonella Rossi contributed to the design of the study, performed the lymphatic staining and morphometric analysis, and contributed to the writing. E.R., E.W., D.J.A., A.U.W. contributed to the study design, data interpretation and writing/revision of the manuscript. E.W. also supervised the immunohistochemistry staining and analysis. P.S. contributed to the study design, performed the data analysis and contributed to writing/revision of the manuscript.

References

Aurora AB, Baluk P, Zhang D, et al. (2005) Immune complex-dependent remodelling of the airway vasculature in response to a chronic bacterial infection. *J Immunol* **175**, 6319–6326.

Baluk P, Tammela T, Ator E, et al. (2005) Pathogenesis of persistent lymphatic vessel hyperplasia in chronic airway inflammation. *J Clin Invest* **115**, 247–257.

Bonsib SM (2006) Renal lymphatics, and lymphatic involvement in sinus vein invasive (pT3b) clear cell renal cell carcinoma: a study of 40 cases. *Mod Pathol* **19**, 746–753.

Comparini L (1969) Lymph vessels of the liver in man. *Angiologica* **6**, 262–274.

Corrin B, Nicholson AG, Rice A (2011) *Pathology of the Lungs, Chapter 14*, 3rd edn. Edinburgh: Churchill Livingstone Elsevier, p. 756.

Cox EP (1927) A method of assigning numerical and percentage values to the degree of roundness of sand grains. *J Paleontol* **1**, 179–183.

Ebina M (2008) Remodeling of airway walls in fatal asthmatics decreases lymphatic distribution; beyond thickening of airway smooth muscle layers. *Allergol Int* **57**, 165–174.

Ebina M, Shibata N, Ohta H, et al. (2010) The disappearance of pleural and interlobular lymphatics in idiopathic pulmonary fibrosis. *Lymphat Res Biol* **8**, 199–207.

El Chemaly S, Levine SJ, Moss J (2008) Lymphatics in lung disease. *Ann N Y Acad Sci* **1131**, 195–202.

El-Chemaly S, Malide D, Zudaire E, et al. (2009) Abnormal lymphangiogenesis in idiopathic pulmonary fibrosis with insights into cellular and molecular mechanisms. *Proc Natl Acad Sci U S A* **106**, 3958–3963.

Feiveson AH (2002) Power by simulation. *Stata J* **2**, 107–124.

Hansell DM, Bankier AA, MacMahon H, et al. (2008) Fleischner Society: glossary of terms for thoracic imaging. *Radiology* **246**, 697–722.

Hirakawa S, Hong YK, Harvey N, et al. (2003) Identification of vascular lineage-specific genes by transcriptional profiling of isolated blood vascular and lymphatic endothelial cells. *Am J Pathol* **162**, 575–586.

Jurisic G, Detmar M (2009) Lymphatic endothelium in health and disease. *Cell Tissue Res* **335**, 97–108.

Kahn HJ, Marks A (2002) A new monoclonal antibody, D2-40, for detection of lymphatic invasion in primary tumors. *Lab Invest* **82**, 1255–1257.

Kambouchner M, Bernaudin J (2009) Intralobular pulmonary lymphatic distribution in normal human lung using D2-40 antipodoplanin immunostaining. *J Histochem Cytochem* **57**, 643–648.

Kambouchner M, Pirici D, Uhl JF, et al. (2011) Lymphatic and blood microvasculature organisation in pulmonary sarcoid granulomas. *Eur Respir J* **37**, 835–840.

Karagiannis A, Gallopin T, Dávid C, et al. (2009) Classification of NPY-expressing neocortical interneurons. *J Neurosci* **18**, 3642–3659.

Kato S, Shimoda H, Ji R-C, et al. (2006) Lymphangiogenesis and expression of specific molecules as lymphatic endothelial cell markers. *Anat Sci Int* **81**, 71–83.

Kriehuber E, Breiteneder-Geleff S, Groeger M, et al. (2001) Isolation and characterization of dermal lymphatic and blood endothelial cells reveal stable and functionally specialized cell lineages. *J Exp Med* **194**, 797–808.

Kulkarni RM, Herman A, Ikegami M, et al. (2011) Lymphatic ontogeny and effect of hypoplasia in developing lung. *Mech Dev* **128**, 29–40.

Lai Fook SJ (2004) Pleural mechanics and fluid exchange. *Physiol Rev* **84**, 385–410.

Lauweryns JM, Baert JA (1977) Alveolar clearance and the role of the pulmonary lymphatics. *Am Rev Resp Dis* **115**, 625–683.

Lee H-W, Qin Y-X, Kim Y-M, et al. (2011) Expression of lymphatic endothelium-specific hyaluronan receptor LYVE-1 in the developing mouse kidney. *Cell Tissue Res*, **343**, 429–444.

Mandal RV, Mark EJ, Kradin RL (2008) Organizing pneumonia and pulmonary lymphatic architecture in diffuse alveolar damage. *Hum Pathol* **39**, 1234–1238.

Marchetti C, Poggi P, Clement MG, et al. (1994) Lymphatic capillaries of the pig lung: TEM and SEM observations. *Anat Rec* **238**, 368–373.

Miserocchi G, Negrini D, Passi A, et al. (2001) Development of lung edema: interstitial fluid dynamics and molecular structure. *News Physiol Sci* **16**, 66–71.

Mote VL, Anderson RL (1965) An investigation of the effect of misclassification on the properties of chi-square tests in the analysis of categorical data. *Biometrica* **52**, 95–109.

Negrini D, Passi A (2007) Interstitial matrix and transendothelial fluxes in normal lung. *Respir Physiol Neurobiol* **159**, 301–310.

Ohtani O, Ohtani Y (2008) Organization and developmental aspects of lymphatic vessels. *Arch Histol Cytol* **71**, 1–22.

O'Morchoe CC (1997) Lymphatic system of the pancreas. *Microsc Res Tech* **37**, 456–477.

Partanen TA, Arola J, Saaristo A, et al. (2000) VEGF-C and VEGF-D expression in neuroendocrine cells and their receptor, VEGFR-3, in fenestrated blood vessels in human tissues. *FASEB J* **14**, 2087–2096.

Rossi A, Sozio F, Sestini P, et al. (2010) Lymphatic and blood vessels in scleroderma skin, a morphometric analysis. *Hum Pathol* **41**, 366–374.

Scavelli C, Weber E, Aglianò M, et al. (2004) Lymphatics at the crossroads of angiogenesis and lymphangiogenesis. *J Anat* **204**, 433–449.

Schermuly RT, Dony E, Ghofrani HA, et al. (2005) Reversal of experimental pulmonary hypertension by PDGF inhibition. *J Clin Invest* **115**, 2811–2821.

Schraufnagel DE (2010) Lung lymphatic anatomy and correlates. *Pathophysiology* **17**, 337–343.

Sokal RR (1974) Classification: purposes, principles, progress, prospects. *Science* **185**, 1115–1123.

Wick N, Haluza D, Gurnhofer E, et al. (2008) Lymphatic precollectors contain a novel, specialized subpopulation of podoplanin low, CCL27-expressing lymphatic endothelial cells. *Am J Pathol* **173**, 1202–1209.

Yamashita M, Iwama N, Date F, et al. (2009) Characterization of lymphangiogenesis in various stages of idiopathic diffuse alveolar damage. *Hum Pathol* **40**, 542–551.

Zocchi L (2002) Physiology and pathophysiology of pleural fluid turnover. *Eur Resp J* **20**, 1545–1558.

Supporting Information

Additional Supporting Information may be found in the online version of this article:

Fig. S1. Histograms of the distribution of log-transformed perimeter (left) and area (right) in different populations of lymphatic vessels.

Fig. S2. Histogram of the distribution of elongation in different populations of lymphatic vessels.

Fig. S3. Scree plot of the fraction of total variance in the data as explained or represented by each of the seven principal components resulting from the analysis.

Table S1. Morphometric measurements of perivascular lymphatics.

Table S2. The eigenvectors of the four components retained in the model.

As a service to our authors and readers, this journal provides supporting information supplied by the authors. Such materials are peer-reviewed and may be re-organized for online delivery, but are not copy-edited or typeset. Technical support issues arising from supporting information (other than missing files) should be addressed to the authors.